

# Electronic states in the quantum-wire network of moiré bilayer systems

(& a brief overview)

徐晨軒

Chen-Hsuan Hsu

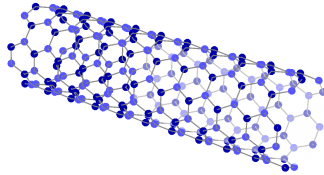
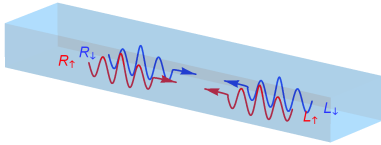
QMP group, IoP, AS

2023 IoP mini workshop

August 2nd, 2023

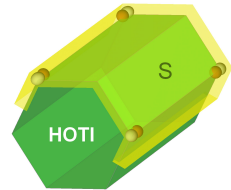
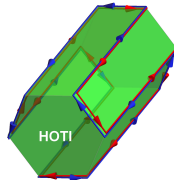
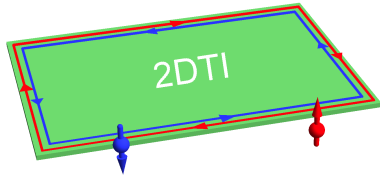
# Research interests

- Quantum matter and quantum phenomena in nanoscale systems (theory)
- Nanowires or nanotubes



[CHH et al., PRB 92, 235435 \(2015\)](#); [CHH et al., PRB 100, 195423 \(2019\)](#); [CHH et al., PRR 2, 043208 \(2020\)](#)

- Topological materials: two-dimensional (2D) or higher-order (HO) topological insulators (TI)

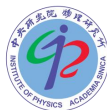


[CHH et al., PRB 96, 081405\(R\) \(2017\)](#); [CHH et al., PRL 121, 196801 \(2018\)](#); [CHH et al., SST 36, 123003 \(2021\)](#)

# Active collaborations and ongoing research

- 1D or quasi-1D systems
  - Daniel Loss (Basel & RIKEN)
  - Jelena Klinovaja (Basel)
  - Yung-Yeh Chang (AS postdoc prog, 2023/8~)
  - Hao-Chien Wang (assistant)
- Numerical modeling on QSHI
  - Hsin Lin
  - Li-Shao Chiang (assistant)
- Solitons in topological systems
  - Hsin Lin
  - Yi-Chun Hung (student, Northeastern University)
- IoP Summer Student Internship
  - Yu-Peng Wang (student, NTHU)
  - Yu-Ren Lai (student, NCU)
  - Kuan-Lin Kuo (student, CYU)

• Fundings:



# Outline

Unconventional states of matter in moiré bilayer systems

2D triangular network in moiré systems

Electronic states in 2D network of interacting quantum wires

# Outline

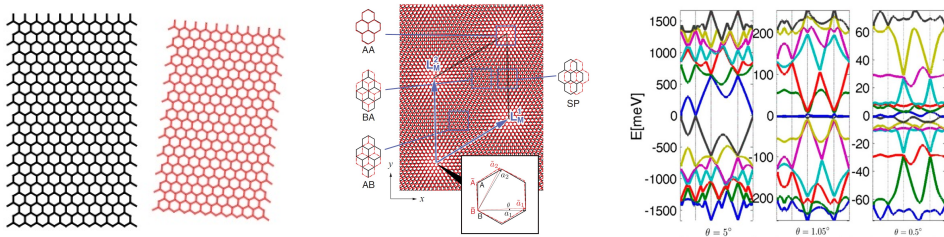
Unconventional states of matter in moiré bilayer systems

2D triangular network in moiré systems

Electronic states in 2D network of interacting quantum wires

# 2D twisted structures

- Twist angle between 2D monolayers:  
a tunable parameter allowing for continuously varying the band structure  
⇒ band-structure engineering



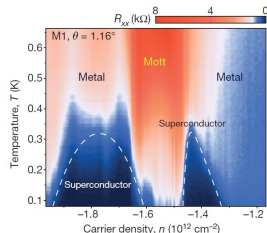
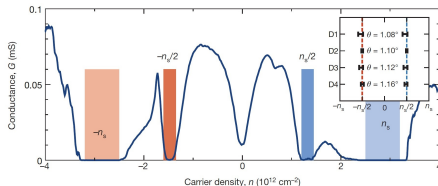
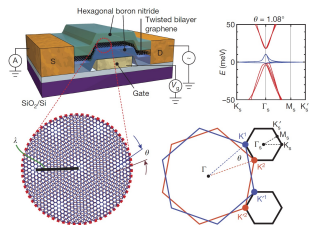
Nam and Koshino, PRB 2017

Bistritzer and MacDonald, PNAS 2011

- Moiré pattern with wavelength  $\lambda = a_0/[2 \sin(\theta/2)]$ 
  - $\theta$ : twist angle between layers;  $a_0$ : lattice constant of graphene monolayer
  - $\lambda \approx 13$  nm for  $a_0 = 0.246$  nm and  $\theta = 1.1^\circ$
- (Quasi-)flat bands close to the magic angle ( $e$ - $e$  interaction  $>$  bandwidth  $\approx$  kinetic energy)  
⇒ a platform for strongly correlated electron systems

# Strongly correlated systems in twisted bilayer graphene

- Magic-angle twisted bilayer graphene (TBG)



Cao et al., Nature 556, 43 (2018); Cao et al., Nature 556, 80 (2018)

- Carrier density electrically tuned by voltage gate
- Band insulator for 4e (or 4h) per moiré unit cell and semimetal at charge neutrality point
- Unconventional states of matter when the Fermi energy lies within the (quasi-)flat bands
- Phase diagram: resembling high-T<sub>c</sub> materials
  - (Mott-like) correlated insulating phase at half filling (both flat bands)
  - dome-like superconductivity regions in e- and h-doped sides of Mott phase (lower flat band)
- Earlier study on moiré pattern and electronic structure of MoS<sub>2</sub>/WSe<sub>2</sub> heterobilayers  
Zhang et al., Sci. Adv. 3, 1601459 (2017)

# Subsequent observations of correlated insulator and superconductor

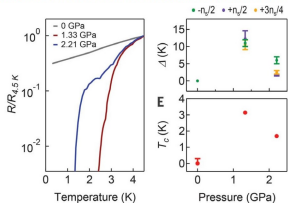
RESEARCH

## RESEARCH ARTICLE

SUPERCONDUCTIVITY

### Tuning superconductivity in twisted bilayer graphene

Matthew Yankowitz<sup>1\*</sup>, Shaowen Chen<sup>1,2\*</sup>, Hryhorii Polshyn<sup>3\*</sup>, Yuxuan Zhang<sup>3</sup>, K. Watanabe<sup>4</sup>, T. Taniguchi<sup>4</sup>, David Graf<sup>5</sup>, Andrea F. Young<sup>6,†</sup>, Cory R. Dean<sup>1,†</sup>

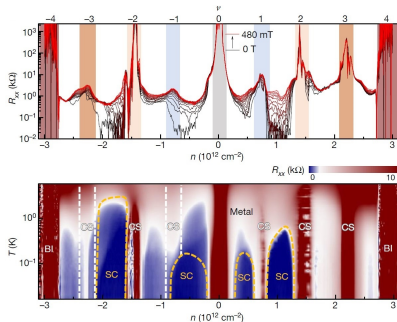


Yankowitz et al., Science 2019

Article

### Superconductors, orbital magnets and correlated states in magic-angle bilayer graphene

<https://doi.org/10.1038/s41566-019-1695-0> Xiaobo Lu<sup>1</sup>, Petr Stepanov<sup>1</sup>, Wei Yang<sup>1</sup>, Ming Xie<sup>1</sup>, Mohamad Ali Azeem<sup>1</sup>, Iqbal Das<sup>1</sup>, Carlos Dreyer<sup>2</sup>, Kengji Watanabe<sup>3</sup>, Takashi Taniguchi<sup>3</sup>, Guangyu Zhang<sup>4</sup>, Adrian Bachtold<sup>5</sup>, Allan H. MacDonald<sup>6</sup> & Dmitri K. Efetov<sup>1\*</sup>  
Received: 16 March 2019  
Accepted: 12 August 2019



Lu et al., Nature 2019

- More robust electronic states in samples with reduced inhomogeneity
  - pressure-enhanced superconductivity and correlated insulator
  - correlated insulating phases also at 1/4 and 3/4 fillings (both flat bands)
  - superconductivity domes (both flat bands) with  $T_c$  up to 3 K

# Anomalous Hall effect in TBG

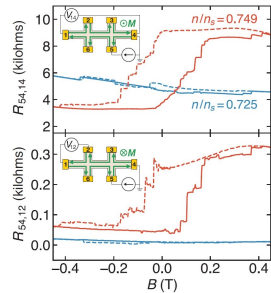
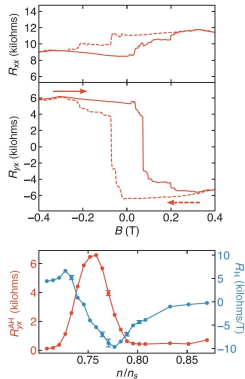
RESEARCH

GRAPHENE

## Emergent ferromagnetism near three-quarters filling in twisted bilayer graphene

Aaron L. Sharpe<sup>1,2,\*</sup>, Eli J. Fox<sup>2,3,\*</sup>, Arthur W. Barnard<sup>3</sup>, Joe Finney<sup>3</sup>, Kenji Watanabe<sup>4</sup>, Takashi Taniguchi<sup>4</sup>, M. A. Kastner<sup>2,3,5,6</sup>, David Goldhaber-Gordon<sup>2,3,†</sup>

When two sheets of graphene are stacked at a small twist angle, the resulting flat superlattice minibands are expected to strongly enhance electron-electron interactions. Here, we present evidence that near three-quarters ( $3/4$ ) filling of the conduction miniband, these enhanced interactions drive the twisted bilayer graphene into a ferromagnetic state. In a narrow density range around an apparent insulating state at  $3/4$ , we observe emergent ferromagnetic hysteresis, with a giant anomalous Hall (AH) effect as large as 10.4 kilohms and indications of chiral edge states. Notably, the magnetization of the sample can be reversed by applying a small direct current. Although the AH resistance is not quantized, and dissipation is present, our measurements suggest that the system may be an incipient Chern insulator.



Sharpe et al., Science 2019

- TBG nearly aligned to the top hBN layer
- Ferromagnetic hysteresis with a coercive field  $B \sim O(0.1 \text{ T})$  at  $3/4$  filling for  $T < 3.9 \text{ K}$
- Large Hall resistance and chiral edge modes at  $B = 0$  (upper flat band)
- Possible indication of the existence of topological phases

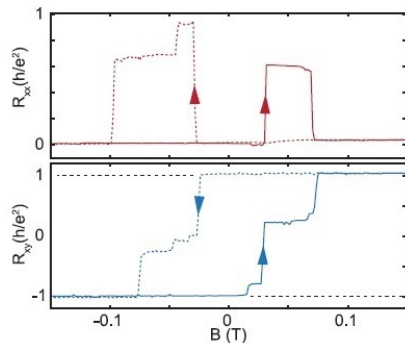
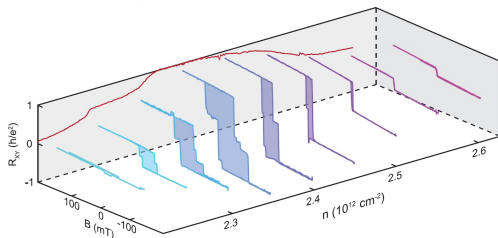
# Experimental indication of topological matter in TBG

RESEARCH

TOPOLOGICAL MATTER

## Intrinsic quantized anomalous Hall effect in a moiré heterostructure

M. Serlin<sup>1\*</sup>, C. L. Tschirhart<sup>1\*</sup>, H. Polshyn<sup>1\*</sup>, Y. Zhang<sup>1</sup>, J. Zhu<sup>1</sup>, K. Watanabe<sup>2</sup>, T. Taniguchi<sup>2</sup>, L. Balents<sup>3</sup>, A. F. Young<sup>1†</sup>



Serlin et al., Science 2020

- Quantized Hall resistance  $R_{xy} = h/e^2$  at 3/4 filling at  $B = 0$ ,  $T = 1.6$  K in TBG aligned to hBN  $\Rightarrow$  quantum anomalous Hall insulator (QAHI) or Chern insulator with Chern number  $C = 1$

# Subsequent observations of QAHI or Chern insulator in TBG

- A sequence of Chern insulator states with Chern number  $C = \pm 1, \pm 2$  and  $\pm 3$  observed at the filling factor  $\nu = \pm 3/4, \pm 2/4$  and  $\pm 1/4$ , respectively
    - complete sequence: Nuckolls et al., Nature 2020; Choi et al., Nature 2021; Das et al., Nat. Phys. 2021
    - partial sequence: Park et al., Nature 2021; Saito et al., Nat. Phys. 2021; Stepanov et al., PRL 2021; Lin et al., Science 2022; Tseng et al., Nat. Phys. 2022
- ⇒ topologically nontrivial phases as a common feature across samples and setups

## Strongly correlated Chern insulators in magic-angle twisted bilayer graphene

<https://doi.org/10.1038/s41586-020-3028-8>  
Received: 3 July 2020

Kevin F. Nuckolls<sup>1,5</sup>, Myungchul Oh<sup>1,5</sup>, Dillon Wong<sup>1,5</sup>, Biao Lian<sup>1</sup>, Kenji Watanabe<sup>2</sup>, Takashi Taniguchi<sup>2</sup>, B. Andrei Bernevig<sup>1</sup> & Ali Yazdani<sup>1,2</sup>

LETTERS

<https://doi.org/10.1038/s41586-020-3028-8>

nature  
physics

Article

Symmetry-broken Chern insulators and Rashba-like Landau-level crossings in magic-angle bilayer graphene

Jeeha Das<sup>1</sup>, Xiaobo Lu<sup>1,2,5</sup>, Jonah Herzog-Arbeitman<sup>1</sup>, Zhi-Da Song<sup>1</sup>, Kenji Watanabe<sup>2</sup>, Takashi Taniguchi<sup>2</sup>, B. Andrei Bernevig<sup>1</sup> and Dmitri K. Efetov<sup>1,2</sup>

<https://doi.org/10.1038/s41586-021-03366-w>  
Received: 26 August 2020

Jeong Min Park<sup>1,4</sup>, Yuan Cao<sup>1,4,5</sup>, Kenji Watanabe<sup>2</sup>, Takashi Taniguchi<sup>2</sup> & Pablo Jarillo-Herrero<sup>1,2</sup>

PHYSICAL REVIEW LETTERS 127, 197701 (2021)

Editors' Suggestion

Competing Zero-Field Chern Insulators in Superconducting Twisted Bilayer Graphene

Petr Stepanov<sup>1,17</sup>, Ming Xie<sup>2</sup>, Takashi Taniguchi<sup>2</sup>, Kenji Watanabe<sup>2</sup>, Xiaobo Lu<sup>1</sup>, Allan H. MacDonald<sup>2</sup>, B. Andrei Bernevig<sup>1</sup> and Dmitri K. Efetov<sup>1,17</sup>

## Correlation-driven topological phases in magic-angle twisted bilayer graphene

<https://doi.org/10.1038/s41586-020-03159-7>  
Received: 21 August 2020

Youngjoon Choi<sup>1,3,5</sup>, Hyunjin Kim<sup>1,3,5</sup>, Yang Peng<sup>1</sup>, Alex Thomson<sup>1,3,5</sup>, Cyrtan Leseandrowski<sup>1,3,5</sup>, Robert Polak<sup>1,3</sup>, Yiran Zhang<sup>1,3</sup>, Harpreet Singh Arora<sup>1,3</sup>, Kenji Watanabe<sup>2</sup>, Takashi Taniguchi<sup>2</sup>, Jason Alicea<sup>2,4</sup> & Stevan Nadj-Perga<sup>1,2,5</sup>

LETTERS

<https://doi.org/10.1038/s41586-020-03159-7>

nature  
physics

Hofstadter subband ferromagnetism and symmetry-broken Chern insulators in twisted bilayer graphene

Yu Saito<sup>1,4</sup>, Jingyuan Gu<sup>1</sup>, Louk Rademaker<sup>1</sup>, Kenji Watanabe<sup>2</sup>, Takashi Taniguchi<sup>2</sup>, Dmitry A. Abanin<sup>1</sup> and Andrus F. Young<sup>1,2</sup>

RESEARCH

2D MATERIALS

Spin-orbit-driven ferromagnetism at half moiré filling in magic-angle twisted bilayer graphene

Jiang-Xiui Liu<sup>1</sup>, Yi-Nai Zhang<sup>1</sup>, Erin Morissette<sup>1</sup>, Zhi Wang<sup>1</sup>, Song Liu<sup>1</sup>, Daniel Rhodes<sup>1</sup>, K. Watanabe<sup>2</sup>, T. Taniguchi<sup>2</sup>, James Hone<sup>1</sup>, J. I. A. Li<sup>1,4</sup>

LETTERS

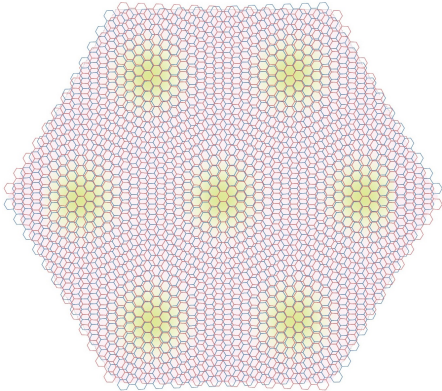
<https://doi.org/10.1038/s41586-020-03159-7>

nature  
physics

Anomalous Hall effect at half filling in twisted bilayer graphene

Chan-Chih Tsung<sup>1</sup>, Xiaotao Ma<sup>1,5</sup>, Zhaoyu Liu<sup>1,5</sup>, Kenji Watanabe<sup>2</sup>, Takashi Taniguchi<sup>2</sup>, Jun-Ho Chu<sup>1</sup> and Matthew Yankowitz<sup>1,2,5</sup>

# Challenge for theoretical analysis



Cao et al., Science 2021

- Experimental observations of unconventional electronic states in TBG motivated numerous theoretical works
- Correlation: beyond single-particle picture
- Challenge:  
large number of atoms  $\sim O(10^4)$  due to large moiré unit cells
- To develop tractable analytic tools, a theoretical framework identifying relevant degrees of freedom is highly desirable!

# Outline

Unconventional states of matter in moiré bilayer systems

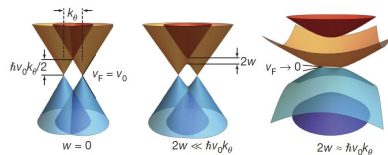
**2D triangular network in moiré systems**

Electronic states in 2D network of interacting quantum wires

# Continuum model for TBG

- Single-particle Hamiltonian: hybridization of Dirac cones in the two layers

$$H_{\text{sp}} = \begin{pmatrix} H_{\gamma\sigma}^{(t)} & T_{\gamma}(\mathbf{x}) \\ T_{\gamma}^{\dagger}(\mathbf{x}) & H_{\gamma\sigma}^{(b)} \end{pmatrix}$$



Cao et al., Nature 2018

- basis:  $(c_{A\gamma\sigma}^t, c_{B\gamma\sigma}^t, c_{A\gamma\sigma}^b, c_{B\gamma\sigma}^b)^T$
- Dirac Hamiltonian for the TBG with a twist angle  $\theta$ :

$$H_{\gamma\sigma}^{(\eta)} = \begin{pmatrix} -\eta V_d & \gamma \hbar v_F |\mathbf{k}| e^{-i\gamma(\theta_k - \eta\theta/2)} \\ \gamma \hbar v_F |\mathbf{k}| e^{i\gamma(\theta_k - \eta\theta/2)} & -\eta V_d \end{pmatrix}$$

- $\theta_k$ : angle of the momentum direction;  $V_d$ : interlayer bias;  $\eta$ : layer index;  $\gamma$ : valley index
- Interlayer hybridization (with the 2D coordinate  $\mathbf{x}$ ):

$$T_{\gamma}(\mathbf{x}) = \frac{w}{3} \sum_{j=1}^3 e^{i\gamma \mathbf{q}_j \cdot (\mathbf{x} + \mathbf{x}_0)} T_{\gamma,j}, \quad T_{\gamma,1} = \begin{pmatrix} 1 & 1 \\ 1 & 1 \end{pmatrix}, \quad T_{\gamma,2} = (T_{\gamma,3})^* = \begin{pmatrix} e^{i2\gamma\pi/3} & 1 \\ e^{-i2\gamma\pi/3} & e^{i2\gamma\pi/3} \end{pmatrix}$$

- $\mathbf{q}_1 \equiv -k_{\theta} \mathbf{e}_y$ ,  $\mathbf{q}_2 \equiv k_{\theta} (\frac{\sqrt{3}}{2} \mathbf{e}_x + \frac{1}{2} \mathbf{e}_y)$ ,  $\mathbf{q}_3 \equiv k_{\theta} (-\frac{\sqrt{3}}{2} \mathbf{e}_x + \frac{1}{2} \mathbf{e}_y)$ , and  $k_{\theta} \equiv \frac{8\pi}{3a_0} \sin(\theta/2)$

Bitrizer and MacDonald, PNAS 2011; Efimkin and MacDonald, PRB 2018

## Low-energy effective model

- For sufficiently large  $V_d$ , the continuum model  $H_{sp}$  can be projected onto the conduction band of the top layer and the valence band of the bottom layer
- Low-energy effective model: describing massive Dirac fermion

$$\begin{pmatrix} \hbar v_F |\mathbf{k}| & -\gamma \Delta_- \cos \theta_k - i \Delta_+ \sin \theta_k \\ -\gamma \Delta_- \cos \theta_k + i \Delta_+ \sin \theta_k & -\hbar v_F |\mathbf{k}| \end{pmatrix}$$

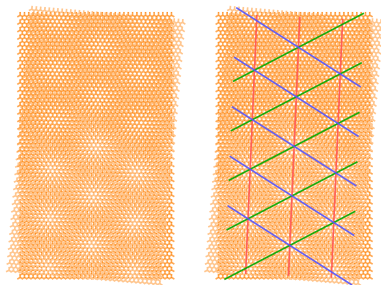
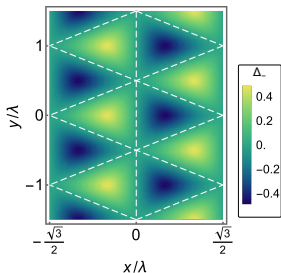
- effective mass from the interlayer hybridization:

$$\Delta_{\pm, \gamma} \equiv \frac{|T_{\gamma}^{AB}| \pm |T_{\gamma}^{BA}|}{2}$$
$$\phi_{\pm, \gamma} \equiv \frac{\arg(T_{\gamma}^{AB}) \pm \arg(T_{\gamma}^{BA})}{2}$$

- spatial dependence in  $\Delta_-$ : a spatially dependent sign of mass (i.e., spectral gap)
- mapped to a  $(p_x \pm ip_y)$  superconductor:
  - $\Rightarrow$  gapless modes between domains with opposite mass set by  $\text{sign}(\gamma \Delta_-)$

# Triangular network of domain walls in TBG

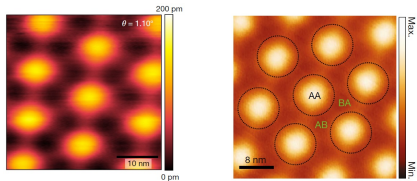
- Spatial profile of  $\Delta_-$ : following moiré pattern of TBG



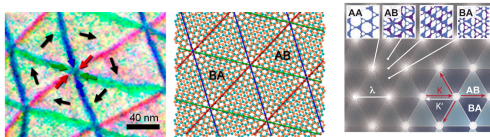
- $\text{sign}(\Delta_-)$ : opposite signs of effective mass in neighboring domains
- dashed lines: domain walls separating domains with the opposite sign of  $(\Delta_-)$
- Low-energy solutions (Jackiw-Rebbi problem):  
⇒ gapless modes emerge at domain walls between AB- and BA-stacking regions
- 2D triangular network formed by 1D conduction channels along domain walls  
[San-Jose and Prada, PRB 2013](#); [Nam and Koshino, PRB 2017](#); [Efimkin and MacDonald, PRB 2018](#)

# 2D network or array of 1D channels in TBG and similar nanostructures

- STM/TEM/transport features of domain-wall modes between AB- and BA-stacking areas

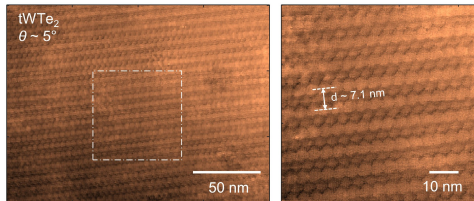


Kerelsky et al., Nature 2019; Jiang et al., Nature 2019



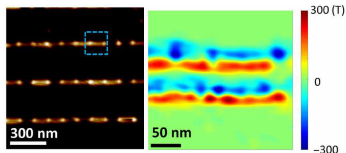
Alden et al., PNAS 2013; Rickhaus et al., Nano Lett. 2018

- Arrays of 1D channels in other 2D materials
  - twisted  $\text{WTe}_2$



Wang et al., Nature 2022; Yu et al., arXiv:2307.15881

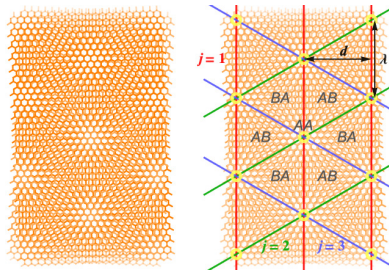
- strain-engineered graphene



Hsu et al., Sci. Adv. 6, aat9488 (2020)

# Incorporating $e-e$ interactions in 2D network of moiré bilayer systems

- 2D network of interacting quantum wires at nanoscales:



- Unconventional states of matter in 1D or quasi-1D systems:
  - interacting electrons in 1D: (Tomonaga-)Luttinger liquid (TLL)
  - coupled parallel interacting wires: sliding TLL
    - ⇒ intrawire and interwire forward scattering of  $e-e$  interactions on equal footing
  - triangular network of 1D wires: 3 sets of sliding TLL

Wu et al., PRB 2019; Chen et al., PRB 2020; Chou et al., PRB 2021

\*related work on square network: Chou et al., PRB 2019

# Outline

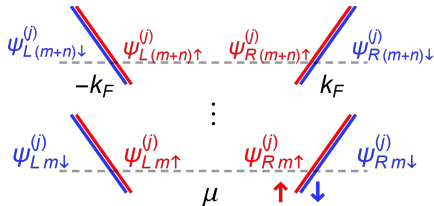
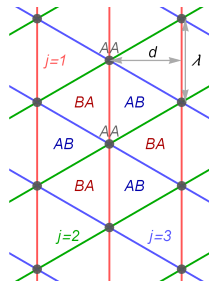
Unconventional states of matter in moiré bilayer systems

2D triangular network in moiré systems

Electronic states in 2D network of interacting quantum wires

## 2D network formed by gapless domain wall modes

- Electrons in 2D network consisting of interacting quantum wires
- Fermion field operator  $\psi_{\ell m \sigma}^{(j)}(x)$ :
  - array index  $j \in \{1, 2, 3\}$
  - wire index  $m \in [1, N_{\perp}]$  within each array
  - moving direction along the wire  $\ell \in \{R \equiv +, L \equiv -\}$
  - spin  $\sigma \in \{\uparrow \equiv +, \downarrow \equiv -\}$
  - local coordinate  $x$  along the wire
- Parallel wires within an array:
  - chemical potential  $\mu$  and Fermi wave vector  $k_F$  (identical for all wires)



# Bosonization

- Expressing the fermion field in terms of boson fields:

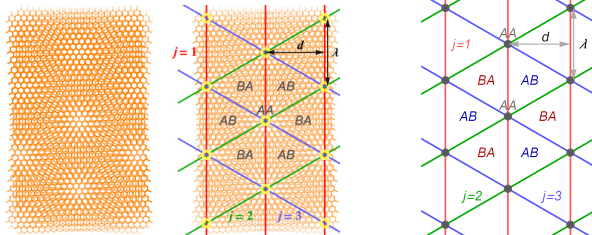
$$\psi_{\ell m \sigma}^{(j)}(x) = \frac{U_{\ell m \sigma}^j}{\sqrt{2\pi a}} e^{i\ell k_F x} e^{\frac{-i}{\sqrt{2}}[\ell\phi_{cm}^j(x) - \theta_{cm}^j(x) + \ell\sigma\phi_{sm}^j(x) - \sigma\theta_{sm}^j(x)]}$$

- $U_{\ell m \sigma}^j$ : Klein factor;  $a$ : short-distance cutoff
- Commutation relation between the boson fields:

$$[\phi_{\xi m}^j(x), \theta_{\xi' m'}^{j'}(x')] = i\frac{\pi}{2} \text{sign}(x' - x) \delta_{jj'} \delta_{\xi\xi'} \delta_{mm'}$$

- index  $\xi, \xi'$  for charge ( $c$ ) or spin ( $s$ ) sector
- charge density operator  $\propto \partial_x \phi_{cm}^j$ ; spin density operator  $\propto \partial_x \phi_{sm}^j$
- charge current operator  $\propto \partial_x \theta_{cm}^j$ ; spin current operator  $\propto \partial_x \theta_{s,m}^j$
- Intrawire or interwire Coulomb (density-density) interaction  $\propto \partial_x \phi_{cm}^j \partial_x \phi_{cn}^j$ 
  - $\Rightarrow$  forward-scattering terms ( $R \leftrightarrow R$  &  $L \leftrightarrow L$ ) in the quadratic form
  - $\Rightarrow$  still diagonalizable

# Bosonized model for the quantum-wire network



- Quantum-wire network with the quadratic interaction terms:

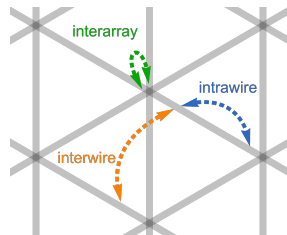
$$H_{0,c}^{(j)} = \sum_{mn} \int \frac{\hbar dx}{2\pi} \left[ V_{\phi,mn}^j \partial_x \phi_{cm}^j \partial_x \phi_{cn}^j + V_{\theta,mn}^j \partial_x \theta_{cm}^j \partial_x \theta_{cn}^j \right]$$

$$H_{0,s}^{(j)} = \sum_n \int \frac{\hbar dx}{2\pi} \left[ \frac{u_s}{K_s} (\partial_x \phi_{sn}^j)^2 + u_s K_s (\partial_x \theta_{sn}^j)^2 \right]$$

- $V_{\phi,mn}^j, V_{\theta,mn}^j, K_s$ : forward-scattering terms ( $R_m \leftrightarrow R_n$  &  $L_m \leftrightarrow L_n$ )
- $\phi_{cn}^j, \theta_{cn}^j, \phi_{sn}^j, \theta_{sn}^j$ : boson fields

# General scattering operator

- Backscatterings ( $R \leftrightarrow L$ ): non-quadratic (sine-Gordon) form
  - analyzed by perturbative renormalization-group (RG) technique
  - potential for various electronic states
- General operator describing various scattering processes:



$$O_{\{s_{\ell p \sigma}^j\}}(x) = \sum_{m=1} \prod_p \prod_j [\psi_{R(m+p)\uparrow}^{(j)}(x)]^{s_{Rp\uparrow}^j} [\psi_{L(m+p)\uparrow}^{(j)}(x)]^{s_{Lp\uparrow}^j} [\psi_{R(m+p)\downarrow}^{(j)}(x)]^{s_{Rp\downarrow}^j} [\psi_{L(m+p)\downarrow}^{(j)}(x)]^{s_{Lp\downarrow}^j}$$

- $\{s_{\ell p \sigma}^j\}$ : integer set for all values of  $(j, \ell, p, \sigma)$  with  $p \in \text{integers}$
- $s \neq 0$  for a given  $p$ : the  $p$ -th nearest neighbor wires participate in the scattering
- physically, we expect  $s \rightarrow 0$  for large  $p$  (finite-range interactions)
- Constraints on  $s_{\ell p \sigma}^j$  due to conservation laws
- Scatterings involving different arrays at intersections:
  - generically allowed but typically less RG relevant
  - we focus on the (intrawire/interwire) scatterings within an array ( $j$  suppressed)

## Constraints on $s_{\ell p\sigma}$ from conservation laws

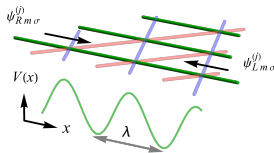
- Condition from global particle number or charge conservation (without “external” pairing):

$$\sum_{p,\sigma} (s_{Rp\sigma} + s_{Lp\sigma}) = 0$$

- Condition from momentum conservation for non-moiré systems:

$$k_F \sum_{p,\sigma} (s_{Rp\sigma} - s_{Lp\sigma}) = 0$$

- In moiré systems, electrons experience a moiré potential with a spatial period of  $\lambda$



$\Rightarrow$  moiré periodic potential provides “crystal momentum”  $\propto$  reciprocal lattice vector  $2\pi/\lambda$

## Unconventional scatterings allowed by moiré periodic potential

- Moiré periodic potential: partially relaxing the constraint from the momentum conservation
- Generalized condition from momentum conservation (for clean systems):

$$k_F \sum_{p,\sigma} (s_{Rp\sigma} - s_{Lp\sigma}) = \frac{2\pi}{\lambda} \times \text{integer}$$

⇒ the momentum difference between the initial and final states of certain scattering processes can be compensated by crystal momentum of moiré potential

⇒ additional processes can take place at certain fillings

- “Resonance condition” from charge conservation and generalized momentum conservation:

$$\nu = \frac{P}{\sum_{p,\sigma} s_{Rp\sigma}}, \quad P \neq 0$$

- filling factor:  $\nu = k_F \lambda / \pi$
- $\nu = 1$  corresponds to 4 electrons per moiré unit cell in TBG
- We refer to this type of processes as *moiré umklapp scatterings*  
⇒ destabilizing the network: *moiré correlated states*

## Examples for moiré umklapp scatterings ( $O_i$ and $O_{ii}$ )

- Further categorized into 4 subtypes:  $O_i$ – $O_{iv}$
- Moiré umklapp scatterings allowed at fractional fillings ( $\nu = P/4$  for illustration)
- $O_i$ : processes involving only intrawire scatterings in individual wires

$$(s_{R0\sigma}, s_{L0\sigma}) \rightarrow (N_\sigma, -N_\sigma)$$

$$N_\sigma \in \mathbb{N}$$

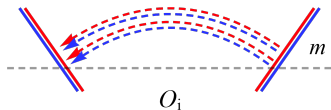
$$O_i = \sum_m (\psi_{Lm\uparrow}^\dagger \psi_{Rm\uparrow})^{N_\uparrow} (\psi_{Lm\downarrow}^\dagger \psi_{Rm\downarrow})^{N_\downarrow}$$

- $O_{ii}$ : processes involving correlated intrawire scatterings in multiple wires

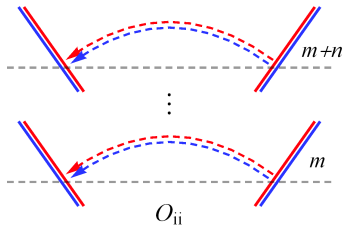
$$(s_{R0\sigma}, s_{L0\sigma}, s_{Rn\sigma}, s_{Ln\sigma}) \rightarrow (N_{0\sigma}, -N_{0\sigma}, N_{n\sigma}, -N_{n\sigma})$$

$$N_{0\sigma}, N_{n\sigma} \in \mathbb{N}$$

$$O_{ii} = \sum_m (\psi_{Lm\uparrow}^\dagger \psi_{Rm\uparrow})^{N_{0\uparrow}} (\psi_{Lm\downarrow}^\dagger \psi_{Rm\downarrow})^{N_{0\downarrow}} \\ \times [\psi_{L(m+n)\uparrow}^\dagger \psi_{R(m+n)\uparrow}]^{N_{n\uparrow}} [\psi_{L(m+n)\downarrow}^\dagger \psi_{R(m+n)\downarrow}]^{N_{n\downarrow}}$$



with  $N_\sigma = 2$



with  $N_{0\sigma} = N_{n\sigma} = 1$

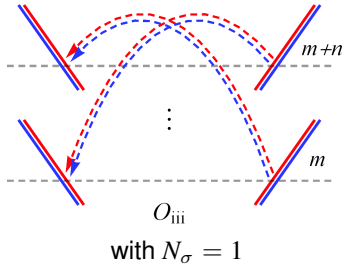
## Examples for moiré umklapp scatterings ( $O_{\text{iii}}$ and $O_{\text{iv}}$ )

- $O_{\text{iii}}$ : processes involving interwire scatterings but still conserving the particle number for each wire

$$(s_{R0\sigma}, s_{L0\sigma}, s_{Rn\sigma}, s_{Ln\sigma}) \rightarrow (N_\sigma, -N_\sigma, N_\sigma, -N_\sigma)$$

$$N_\sigma \in \mathbb{N}$$

$$O_{\text{iii}} = \sum_m [\psi_{L(m+n)\uparrow}^\dagger \psi_{Rm\uparrow}]^{N_\uparrow} [\psi_{L(m+n)\downarrow}^\dagger \psi_{Rm\downarrow}]^{N_\downarrow} \\ \times [\psi_{Lm\uparrow}^\dagger \psi_{R(m+n)\uparrow}]^{N_\uparrow} [\psi_{Lm\downarrow}^\dagger \psi_{R(m+n)\downarrow}]^{N_\downarrow}$$

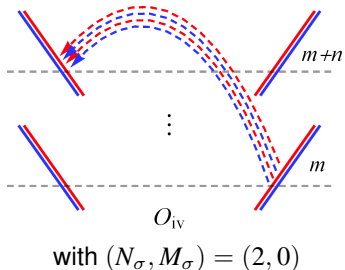


- $O_{\text{iv}}$ : scattering processes that do not conserve particle numbers for individual wires

$$(s_{R0\sigma}, s_{L0\sigma}, s_{Rn\sigma}, s_{Ln\sigma}) \rightarrow (N_\sigma, -M_\sigma, M_\sigma, -N_\sigma)$$

$$N_\sigma, M_\sigma \in \mathbb{N}, \quad N_\sigma \neq M_\sigma$$

$$O_{\text{iv}} = \sum_m [\psi_{L(m+n)\uparrow}^\dagger \psi_{Rm\uparrow}]^{N_\uparrow} [\psi_{L(m+n)\downarrow}^\dagger \psi_{Rm\downarrow}]^{N_\downarrow} \\ \times [\psi_{Lm\uparrow}^\dagger \psi_{R(m+n)\uparrow}]^{M_\uparrow} [\psi_{Lm\downarrow}^\dagger \psi_{R(m+n)\downarrow}]^{M_\downarrow}$$



# Bosonized general scattering operator

- Bosonized form of  $O_{\{s_{\ell p \sigma}\}}$ :

$$O_{\{s_{\ell p \sigma}\}} = \sum_{m=1} \text{Exp} \left\{ \frac{i}{\sqrt{2}} \sum_p [S_{p,c} \phi_{c(m+p)} + \bar{S}_{p,c} \theta_{c(m+p)} + S_{p,s} \phi_{s(m+p)} + \bar{S}_{p,s} \theta_{s(m+p)}] \right\},$$

$$S_{p,\xi} = s_{Lp\uparrow} - s_{Rp\uparrow} + \xi(s_{Lp\downarrow} - s_{Rp\downarrow}),$$

$$\bar{S}_{p,\xi} = s_{Lp\uparrow} + s_{Rp\uparrow} + \xi(s_{Lp\downarrow} + s_{Rp\downarrow}),$$

$$\xi \in \{c \equiv +, s \equiv -\}$$

- Global charge conservation:  $\sum_p \bar{S}_{p,c} = 0$
- Generalized momentum conservation:  $\nu \sum_p S_{p,c} = 2P$ 
  - conventional scatterings:  $P = 0$
  - moiré umklapp scatterings:  $P \in \text{nonzero integer}$
- For processes conserving charge (spin) with a fixed  $p$ :  $\bar{S}_{p,c} (\bar{S}_{p,s}) \rightarrow 0$
- Bosonized  $O_{\{s_{\ell p \sigma}\}}$ : scaling dimensions and RG relevance upon specifying  $V_{\phi, mn}^j$  and  $V_{\theta, mn}^j$ 
  - here we focus on more general (and universal) features

# Systematic construction of moiré umklapp scatterings involving 2 wires

- Fermion form of  $O_i$ – $O_{iv}$  (with  $s_{\ell p\sigma}$  listed below and  $\mathbb{N}$  denoting positive integer):

$$\sum_{m=1} \prod_{p=0} [\psi_{R(m+p)\uparrow}]^{s_{Rp\uparrow}} [\psi_{L(m+p)\uparrow}]^{s_{Lp\uparrow}} [\psi_{R(m+p)\downarrow}]^{s_{Rp\downarrow}} [\psi_{L(m+p)\downarrow}]^{s_{Lp\downarrow}}$$

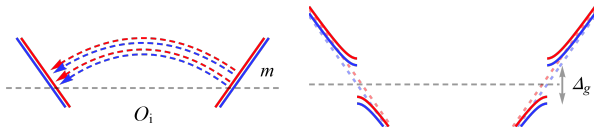
	$s_{\ell p\sigma}$	$\nu$	$S_{p,\xi}$ ( $\xi \in \{c \equiv +, s \equiv -\}$ )
$O_i$	$\ell\delta_{p0}N_\sigma$ , $N_\sigma \in \mathbb{N}$	$\frac{P}{\sum_\sigma N_\sigma}$	$-2\delta_{p0}(N_\uparrow + \xi N_\downarrow)$
$O_{ii}$	$\ell(\delta_{p0} + \delta_{pn})N_{p\sigma}$ , $N_{0\sigma}, N_{n\sigma} \in \mathbb{N}$	$\frac{P}{\sum_\sigma (N_{0\sigma} + N_{n\sigma})}$	$-2(\delta_{p0} + \delta_{pn})(N_{p\uparrow} + \xi N_{p\downarrow})$
$O_{iii}$	$\ell(\delta_{p0} + \delta_{pn})N_\sigma$ , $N_\sigma \in \mathbb{N}$	$\frac{P}{2\sum_\sigma N_\sigma}$	$-2(\delta_{p0} + \delta_{pn})(N_\uparrow + \xi N_\downarrow)$
$O_{iv}$	$\begin{aligned} &\delta_{\ell R}(\delta_{p0}N_\sigma + \delta_{pn}M_\sigma) \quad N_\sigma, M_\sigma \in \mathbb{N}, \\ &-\delta_{\ell L}(\delta_{p0}M_\sigma + \delta_{pn}N_\sigma), \quad N_\sigma \neq M_\sigma \end{aligned}$	$\frac{P}{\sum_\sigma (N_\sigma + M_\sigma)}$	$\begin{aligned} &-2(\delta_{p0} + \delta_{pn})\delta_{\xi c}(N_\uparrow + M_\downarrow) \\ &-2(\delta_{p0} + \delta_{pn})\delta_{\xi s}(N_\uparrow - N_\downarrow) \end{aligned}$

- $\bar{S}_{p,c} = 0$  for  $O_i$ – $O_{iii}$  [CHH et al., arXiv:2303.00759](#)
- $\bar{S}_{p,c} = 2(\delta_{p0} - \delta_{pn})(N_\uparrow - M_\uparrow)$  for  $O_{iv}$
- For simplicity we include examples only for  $\bar{S}_{p,s} = 0$ 
  - operators with a nonzero  $\bar{S}_{p,s}$  are expected to be less RG relevant

## Moiré correlated states at fractional fillings

- $O_i$ – $O_{iii}$ : correlated insulating states with a **fully gapped** system at fractional fillings
- Example:

$$O_i + O_i^\dagger \propto \sum_m \cos(4\sqrt{2}\phi_{cm})$$



$\Rightarrow$  a sum of sine-Gordon terms containing  $\phi_{cm}$  fields

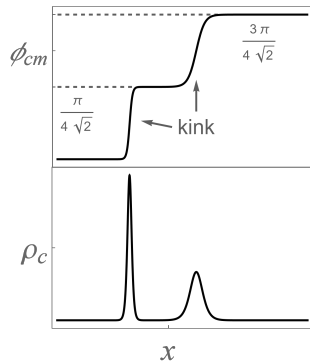
- When  $O_i$  is RG relevant, all the  $\phi_{cm}$  fields are gapped  
 $\Rightarrow$  a fully gapped, correlated insulating state
- $\phi_{cm}$  pinned to minima in the strong-coupling limit:

$$\phi_{cm} \rightarrow \text{odd integer} \times \pi / (4\sqrt{2})$$

- Tunneling between two neighboring minima gives a kink in  $\phi_{cm}$  field:

$$\phi_{cm} \Big|_{\text{kink}+} - \phi_{cm} \Big|_{\text{kink}-} = \pm \pi / (2\sqrt{2})$$

- Spatial derivative  $\partial_x \phi_{cm}$ : related to charge density  $\rho_c$
- **Fractional excitations** with charge  $e/2$  associated with the kink

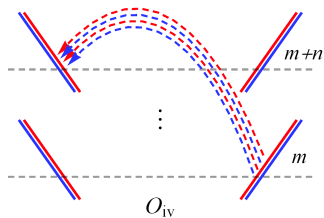


## Gapless chiral edge modes from $O_{iv}$ process

- $\bar{S}_{p,c} \neq 0$  for  $O_{iv}$ : particle number not conserved for individual wires
- Simplest case involving the  $n$ -th nearest neighbor wires:  
 $S_{n,c} = S_{0,c}$ ,  $\bar{S}_{n,c} = -\bar{S}_{0,c}$ , and  $S_{p,c}, \bar{S}_{p,c} = 0$  otherwise
- Introducing chiral fields  $\Phi_{\ell m} = -\ell\phi_{cm} + f\theta_{cm}$  for each wire:

$$[\Phi_{\ell m}(x), \Phi_{\ell' m'}(x')] = i\ell\pi\delta_{\ell\ell'}\delta_{mm'}f \text{sign}(x - x'),$$

$$f = -\bar{S}_{0,c}/S_{0,c}$$



- The perturbation from  $O_{iv}$  process:

$$\delta H_{iv} = g_{iv} \int dx \left( O_{iv} + O_{iv}^\dagger \right) \propto g_{iv} \sum_{m=1} \int dx \cos \left\{ \frac{S_{0,c}}{\sqrt{2}} [\Phi_{L(m+n)} - \Phi_{Rm}] \right\}$$

$\Rightarrow$  involving right- and left-moving modes in the interior of the system

- There remain **gapless chiral modes**:

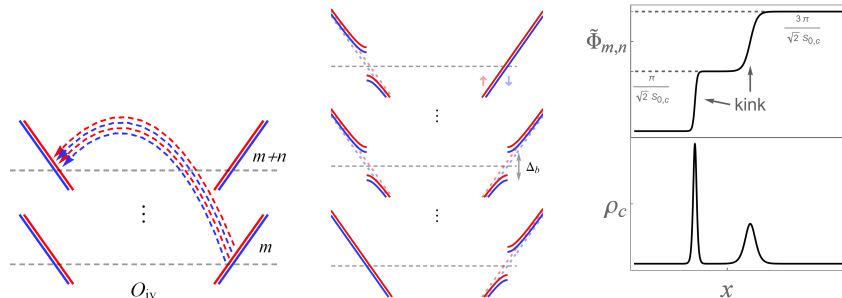
$\Phi_{L,1}, \dots, \Phi_{L,n}$  at one edge and  $\Phi_{R,N_\perp}, \dots, \Phi_{R,(N_\perp - n + 1)}$  at the opposite edge  
 (similarly for the other arrays)

# Fractional excitations

- Defining  $\tilde{\Phi}_{m,n} = [\Phi_{L(m+n)} - \Phi_{Rm}]/2$ :

$$\delta H_{iv} \propto g_{iv} \sum_{m=1} \int dx \cos(\sqrt{2}S_{0,c}\tilde{\Phi}_{m,n})$$

- gapping out bulk modes in the interior of the system  
 $\Rightarrow$  moiré correlated state with an insulating bulk and gapless edge modes



- $\tilde{\Phi}_{m,n}$  pinned to minima:  $\tilde{\Phi}_{m,n} \rightarrow \text{odd integer} \times \pi/(\sqrt{2}S_{0,c})$
- Fractional excitations with charge  $2e/S_{0,c}$  associated with the kink

# Exploring moiré correlated states through gapless edge modes

- At certain fractional fillings,  $O_{iv}$  leads to an insulating bulk with gapless chiral edge modes  
⇒ resembling quantum anomalous Hall effect in TBG
- In the moiré correlated state, the system hosts fractional excitations
- It would be challenging to directly detect the fractional charge  
⇒ probing the moiré correlated state through the edge modes
- Assuming a single mode  $\Phi_{R,N_{\perp}} \rightarrow \phi$  at an edge for simplicity, where the chiral field  $\phi$  satisfies

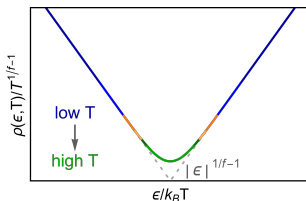
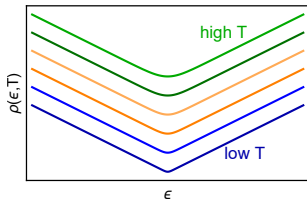
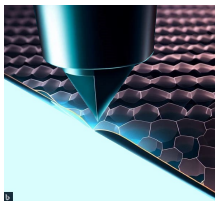
$$[\phi(x), \phi(x')] = i\pi f \text{sign}(x - x')$$

- Effective edge theory from the commutator:

$$\frac{S_{\text{edge}}}{\hbar} = \int \frac{dx d\tau}{4\pi f} \left[ -i\partial_x \phi \partial_{\tau} \phi + v_e (\partial_x \phi)^2 \right]$$

⇒ experimental setups to detect and characterize the edge modes

# Scanning tunneling spectroscopy (STS)



created by Microsoft Image Creator

- Local density of states at the edge:

$$\rho(\epsilon) = \frac{1}{\pi} \text{Re} \left[ \int_0^\infty dt e^{i\epsilon t/\hbar} \langle \psi_e(t) \psi_e^\dagger(0) \rangle \right]$$

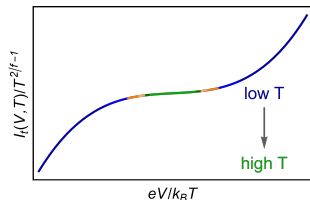
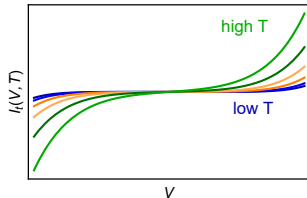
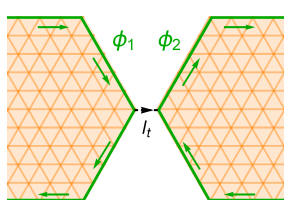
- Universal scaling curve for temperature  $T$  and energy  $\epsilon$  (measured from Fermi level):

$$\rho(\epsilon, T) \propto T^{\frac{1}{f}-1} \cosh \left( \frac{\epsilon}{2k_B T} \right) \left| \Gamma \left( \frac{1}{2f} + i \frac{\epsilon}{2\pi k_B T} \right) \right|^2$$

- power law  $|\epsilon|^{1/f-1}$  at very low  $T$
- scaling parameter determined by universal fraction  $f$ , independent of system details

# Current-bias curve of interedge tunneling

- Proposed edge transport measurement:



- Interedge tunneling process:

$$S_t = t_0 \int d\tau e^{i(\phi_1 - \phi_2)/f}$$

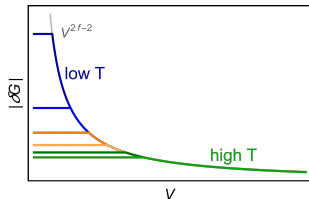
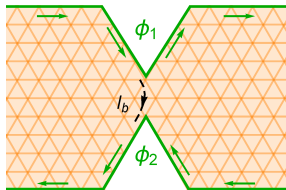
- $t_0$ : non-universal tunnel amplitude
- $\phi_1, \phi_2$ : chiral fields in two separate edges
- Current-bias ( $I_t - V$ ) curve at temperature  $T$ :

$$I_t \propto T^{\frac{2}{f}-1} \sinh\left(\frac{eV}{2k_B T}\right) \left| \Gamma\left(\frac{1}{f} + i\frac{eV}{2\pi k_B T}\right) \right|^2$$

$\Rightarrow$  another universal scaling formula with a scaling parameter set by  $f$

# Conductance correction induced by interedge backscattering

- Proposed edge transport measurement:



- Interedge backscattering process:

$$S_b = v_b \int d\tau e^{i(\phi_1 - \phi_2)}$$

- $v_b$ : non-universal backscattering strength
- $\phi_1, \phi_2$ : chiral fields in two separate edges
- Conductance correction depending on the bias ( $V$ ) and temperature ( $T$ ):

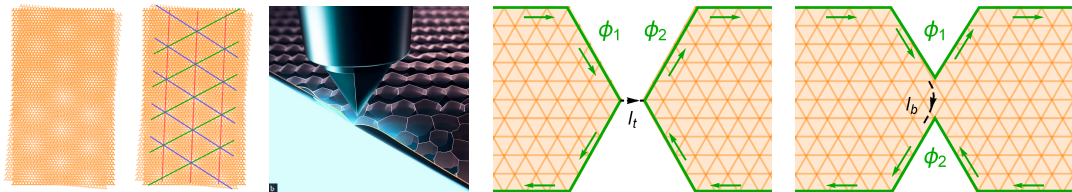
$$|\delta G| \propto \begin{cases} V^{2f-2}, & \text{for } eV \gg k_B T \\ T^{2f-2}, & \text{for } eV \ll k_B T \end{cases}$$

$\Rightarrow$  power-law behavior with a scaling parameter set by  $f$

# Summary

- Bosonic description for general scatterings and electronic states in moiré systems
- Moiré correlated states and fractional excitations from moiré umklapp scatterings
- Correlated states hosting a gapped bulk and gapless edge modes at fractional fillings (resembling quantum anomalous Hall effect observed in experiments)
- Proposed spectroscopic and transport setups for experimental verification

[CHH et al., arXiv:2303.00759](#)



- Outlook:
  - phase diagram from the detailed RG analysis [CHH et al., in preparation](#)
  - further characterization of edge modes through shot noise
  - Majorana and parafermion zero modes with proximity-induced superconductivity

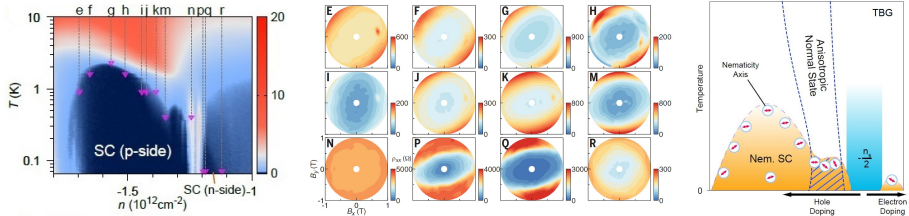
# Nematicity in normal and superconducting states of TBG

RESEARCH

2D MATERIALS

## Nematicity and competing orders in superconducting magic-angle graphene

Yuan Cao<sup>1\*</sup>, Daniel Rodan-Legrain<sup>1</sup>, Jeong Min Park<sup>1</sup>, Noah F. Q. Yuan<sup>1</sup>, Kenji Watanabe<sup>2</sup>, Takashi Taniguchi<sup>3</sup>, Rafael M. Fernandes<sup>4</sup>, Liang Fu<sup>1</sup>, Pablo Jarillo-Herrero<sup>1\*</sup>



Cao et al., Science 2021

- Anisotropic resistivity in the presence of an in-plane magnetic field
- broken rotational symmetry in both normal and superconducting states
- similar features in iron-based superconductors

## Earlier theoretical works on 2D network of TLL

- Earlier works on 2D generalization of coupled Luttinger liquids adopted for cuprates
  - smectic metal or stripe phase  
Emery, Fradkin, Kivelson, and Lubensky, PRL 2000
  - sliding Luttinger liquid  
Vishwanath and Carpentier, PRL 2001
  - crossed sliding Luttinger liquid phase  
Mukhopadhyay, Kane, and Lubensky, PRB(R) 2001
  - 2D and 3D crossed sliding Luttinger liquid phase  
Mukhopadhyay, Kane, and Lubensky, PRB 2001
- Correlated phenomena in 2D investigated using the language of TLL  
⇒ motivation for investigating electronic states in a 2D network of TLL wires
- Instability of (crossed) sliding Luttinger liquids towards various quantum Hall states  
Kane, Mukhopadhyay, and Lubensky, PRL 2002; Klinovaja and Loss, PRL 2013; Sagi and Oreg, PRB 2014;  
Klinovaja and Tserkovnyak, PRB 2014; Teo and Kane, PRB 2014, and more ...

# Recent theoretical works on 2D network of TLL in moiré systems

- Network models related to twisted bilayer systems:
  - coupled-wire construction in the language of conformal field theory  
Wu, Jian, and Xu, PRB 2019
  - the presence of superconducting and correlated insulating phases  
Chou, Lin, Das Sarma, and Nandkishore, PRB 2019
  - generalization to a triangular net of coupled wires  
Chen, Castro Neto, and Pereira, PRB 2020
  - instability towards charge density wave phase  
Chou, Wu, and Sau, PRB 2021
  - non-Fermi liquids  
Lee, Oshikawa, and Cho, PRL 2021
- Existing works on the network model of TBG focused on insulating and superconducting states
- We explore the possibility for topological phases and chiral edge modes in moiré systems

## Conventional scatterings (without relying on moiré potential)

- Scattering processes are generally allowed for any  $k_F$ , provided that

$$\sum_{p,\sigma} (s_{Rp\sigma} - s_{Lp\sigma}) = 0$$

- Together with the particle number conservation  $\sum_{p,\sigma} (s_{Rp\sigma} + s_{Lp\sigma}) = 0$ , we have

$$\sum_{p,\sigma} s_{Rp\sigma} = \sum_{p,\sigma} s_{Lp\sigma} = 0$$

⇒ conservation of the particle number for each moving direction along the wires

- These *conventional scatterings* characterize electronic states independent of fillings  
⇒ “crystalline states” in [Kane et al. PRL 2002](#)
- In moiré systems, the momentum conservation condition is partially relaxed, allowing for scattering processes even when  $\sum_{p,\sigma} s_{Rp\sigma} \neq 0$  or  $\sum_{p,\sigma} s_{Lp\sigma} \neq 0$

# Electronic states due to conventional scatterings

- Electronic states from conventional scatterings:
  - momentum conservation regardless of moiré potential (independent of carrier density)

- Charge density wave coupling

$$(S_{Rp\uparrow}, S_{Lp\uparrow}, S_{Rp\downarrow}, S_{Lp\downarrow}) \rightarrow (-N_{p\uparrow}, N_{p\uparrow}, -N_{p\downarrow}, N_{p\downarrow})$$

$$N_{p\sigma} \in \mathbb{Z}$$

$$O_{\text{cdw}} = \sum_m \prod_p [\psi_{R(m+p)\uparrow}^\dagger \psi_{L(m+p)\uparrow}]^{N_{p\uparrow}} [\psi_{R(m+p)\downarrow}^\dagger \psi_{L(m+p)\downarrow}]^{N_{p\downarrow}}$$

$\Rightarrow$  charge density wave phase when  $O_{\text{cdw}}$  is RG relevant

- Josephson coupling (singlet pairing)

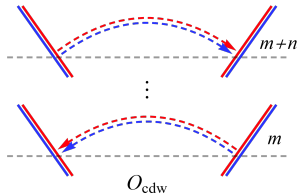
$$(S_{Rp\uparrow}, S_{Lp\uparrow}, S_{Rp\downarrow}, S_{Lp\downarrow}) \rightarrow (-M_p, N_p, N_p, -M_p)$$

$$N_p, M_p \in \mathbb{Z}$$

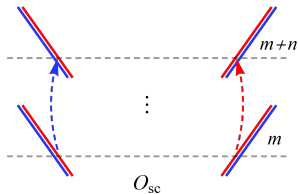
$$O_{\text{sc}} = \sum_m \prod_p [\psi_{R(m+p)\uparrow}^\dagger \psi_{L(m+p)\downarrow}^\dagger]^{M_p} [\psi_{R(m+p)\downarrow} \psi_{L(m+p)\uparrow}]^{N_p}$$

$\Rightarrow$  superconducting phase when  $O_{\text{sc}}$  is RG relevant

- Examined in [Chou et al. PRB 2019](#); [Chen et al. PRB 2020](#)



with  $(N_{0\sigma}, N_{n\sigma}) = (-1, 1)$



with  $(M_0, M_n) = (-1, 1)$